



## An understanding of high entropy alloys from phase diagram calculations



F. Zhang<sup>a,\*</sup>, C. Zhang<sup>a</sup>, S.L. Chen<sup>a</sup>, J. Zhu<sup>a</sup>, W.S. Cao<sup>a</sup>, U.R. Kattner<sup>b</sup>

<sup>a</sup> CompuTherm LLC, Madison, WI, USA

<sup>b</sup> National Institute of Standards and Technology, Gaithersburg, MD, USA

### ARTICLE INFO

#### Article history:

Received 1 August 2013

Received in revised form

16 October 2013

Accepted 31 October 2013

Available online 12 November 2013

#### Keywords:

High entropy alloy

CALPHAD

Multicomponent

Phase diagram calculation

Phase stability

### ABSTRACT

The concept of High Entropy Alloy (HEA) is understood from the point of view of phase diagram calculation. The role of entropy of mixing on the phase stability is discussed for both ideal and non-ideal solid solution phases. The relative stability of a solid solution phase and line compounds is illustrated using hypothetical systems. Calculated binary and multicomponent phase diagrams are used to explain the phenomena observed experimentally for HEAs. The potential of using the CALPHAD (CALCulation of PHase Diagrams) approach in aiding the design of alloys with multiple key components is also discussed.

© 2013 Elsevier Ltd. All rights reserved.

### 1. Introduction

High Entropy Alloys (HEAs) have become a very “hot” topic after Cantor et al. [1] and Yeh et al. [2] published their work in 2004, and publications in this area have increased exponentially since then. HEAs have attracted more and more attention due to their potential beneficial mechanical, magnetic, and electrochemical characteristics, such as high strength, high thermal stability and oxidation resistance. These promising properties offer many potential applications in various fields, such as tools, molds, and magnetic films [2–5]. Among the published work, many studies have focused on the CoCrCuFeNi-based alloys with additions of Al, Ti, and Mn to understand the *fcc/bcc* phase transformation [6–13]. In addition to the use of a traditional trial and error approach, effects of enthalpy of mixing, atomic size difference, and valence electron concentration have been discussed [14,15], and rules have been suggested for the selection of the principal components.

Although development of alloys based on multiple key elements with equal/near equal atomic composition indeed broadened the view of materials scientists/engineers on the design of new materials, the role of entropy of mixing in stabilizing solid solution phases should not be over-emphasized. It is well known that the entropy of mixing can be represented by the following

equation when  $N$  components are randomly mixed together:

$$S_{mix} = -R \sum_i^N x_i \ln x_i \quad (1)$$

where  $x_i$  represents the mole fraction of component  $i$  in the system. The entropy of mixing reaches maximum,  $R \ln N$ , when equal molar amounts of each element are mixed. It should be pointed out that, the definition of Eq. (1) is based on the assumption of random mixing, which does not apply to a phase that forms long-range order or short-range order. Following the paper of Yeh et al. [2], a HEA was defined to contain at least five principal elements with equal/near equal atomic concentration. This paper also indicated that, HEAs tend to form simple solid solution phases instead of multiple intermetallic phases. If entropy of mixing plays a dominant role in the determination of phase stability, it is easy to reach the following conclusions: (1) larger  $N$  would lead to higher probability of forming a HEA, (2) different alloys containing equal number of components would have the same probability of forming a HEA, and (3) equal atomic composition is always more advantageous than non-equal atomic composition in forming a HEA. However, experiments have proved that none of these conclusions are valid [1,16].

Cantor et al. first investigated an alloy consisting of 20 components in equal atomic proportions (mole fraction of 0.05 each), and then an alloy consisting of 16 elements again in equal atomic proportions (mole fraction of 0.0625 each). Both alloys were found to be multiphase and brittle, as-cast and after melt spinning. However, they found both alloys consisted predominantly of a

\* Corresponding author.

E-mail addresses: [fan.zhang@compuTherm.com](mailto:fan.zhang@compuTherm.com) (F. Zhang), [czhang.wisc@gmail.com](mailto:czhang.wisc@gmail.com) (C. Zhang).

single-phase *fcc* primary phase enriched with transition metals Cr, Mn, Fe, Co and Ni. They then casted an alloy with the five components Cr, Mn, Fe, Co and Ni (mole fraction of 0.2 each), and developed a single-phase *fcc* alloy exhibiting a dendritic microstructure. However, when one, two, three, or four elements were added to this five-component system, none of the alloys developed a single-phase *fcc* structure. In summary, in Cantor et al.'s [1] experiments only one alloy, CoCrFeMnNi, was found to form a single-phase *fcc* structure so that increasing the number of key components and, therefore, the entropy of mixing did not help at all in this regard.

In Otto et al.'s paper [16], six alloys were investigated with the base alloy of CoCrFeMnNi. The other five alloys were obtained by replacing one element a time of the base alloy using an element with similar properties of the replaced element. The base alloy was found to consist of a single-phase *fcc* phase, while all the other five alloys consisted of more than one phase.

Obviously, the entropy of mixing does not, at least not always, play a dominant role in the determination of phase stability and therefore the microstructure of an alloy. It is well known that a system reaches its equilibrium state when the total energy of the system reaches the global minimum. The stability of each phase is described by its Gibbs energy which consists of contributions from both enthalpy and entropy. The Gibbs energy is a function of temperature for a line compound phase, a function of temperature and composition for a disordered solution phase, and a function of temperature, composition and site fraction for an ordered intermetallic phase with homogeneity range. The most intuitive way of representing the phase stability in a system is by its phase diagram. When a phase diagram is available, it is not difficult to choose the alloy composition so that a desired microstructure, either a single-phase or a multi-phase mixture, can be developed. In this paper, we will use phase diagram calculation based on the CALPHAD (CALculation of PHase Diagrams) approach [17–19] to understand and explain the microstructures obtained for alloys with multiple key elements. The paper will be arranged as follows: first we will use a hypothetical system to illustrate the relative stability of phases in a system, and the role of entropy in this regard; second we will use calculated binary and multi-component phase diagrams to explain the experimental results obtained in the efforts of developing HEAs, and discuss the role of the CALPHAD approach in aiding the design of HEAs; and last we will summarize our findings and conclusions.

## 2. The role of entropy in the determination of phase stability

In this section, we will discuss the role of entropy in the determination of phase stability using hypothetical systems. Gibbs energy curves (surfaces) will be plotted to demonstrate the phase stability in the composition space. We will first use a hypothetical binary A–B system to show the different roles of entropy of mixing in an ideal and a non-ideal solid solution. We will then extend this binary system to a hypothetical ternary A–B–C system to show the effect of a third component on the relative phase stability of the system. The conclusion obtained in these hypothetical binary and ternary systems can be extended to higher order systems.

### 2.1. Binary A–B system

Let us first use a hypothetical A–B binary system as an example. In Fig. 1, the blue solid line represents the Gibbs energy curve of a disordered solid solution phase, say an *fcc* phase, at one certain temperature. The green solid square and circle represent the Gibbs energies of two line compounds,  $A_{0.75}B_{0.25}$  and  $A_{0.1}B_{0.9}$ , at the same temperature. In this example, A and B form an ideal *fcc* solid

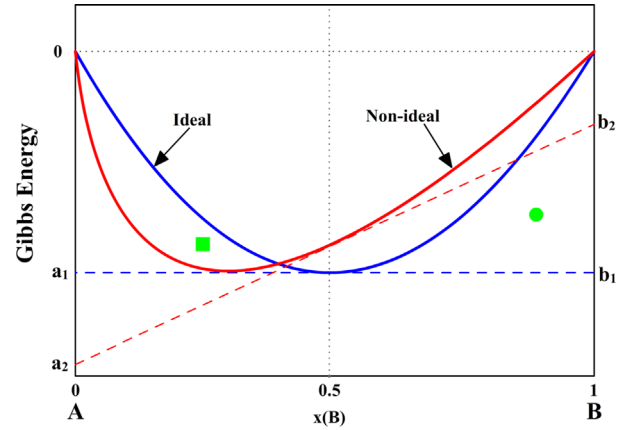


Fig. 1. Gibbs energies of phases in a hypothetical A–B system (For interpretation of the references to color in this figure, the reader is referred to the web version of this article.).

solution (blue curve), i.e., the enthalpy of mixing is zero and the Gibbs energy of the *fcc* phase is represented by

$$G^{fcc} = x_A G_A^{fcc} + x_B G_B^{fcc} + RT(x_A \ln x_A + x_B \ln x_B) \quad (2)$$

When *fcc*-A and *fcc*-B are chosen as the reference states for the plot, the curve starts at zero at the two ends, and reaches the minimum in the middle ( $x_i = 0.5$  for each element). Now if we draw a tangent line ( $a_1b_1$ ) at the composition of equal atomic proportions of A and B, both line compounds are above the line and none of them is stable relative to the ideal solid solution. In this case, the alloy with equal atomic proportions of A and B makes the best choice which favors the formation of single-phase *fcc* phase, and avoids the formation of both line compounds. Slight change of the composition will make the tangent line tilt and one of the two compounds may become stable.

Now, what will happen if A and B do not form an ideal solution? In this case, the Gibbs energy of the *fcc* phase is represented by

$$G^{fcc} = x_A G_A^{fcc} + x_B G_B^{fcc} + RT(x_A \ln x_A + x_B \ln x_B) + G^{ex,fcc} \quad (3)$$

where  $G^{ex,fcc}$  is the excess contribution to the Gibbs energy. In the case of a regular or quasi-regular solution the situation is similar to that of the ideal solution as long as the total Gibbs energy of mixing is negative. However, for subregular solutions the Gibbs energy curve is not symmetric. The Gibbs energy curve of such a non-ideal *fcc* phase is plotted as the red solid line in Fig. 1, and the tangent line at the middle ( $x_i = 0.5$  for each element) is shown by  $a_2b_2$ . In this situation, if equal atomic proportions of A and B are mixed, a mixture of *fcc* and  $A_{0.1}B_{0.9}$  will be obtained instead of single-phase *fcc* phase. In this case, the composition of B cannot exceed 0.3 to obtain a single-phase *fcc* structure.

The conclusions we obtained from this simple hypothetical A–B system are: (1) If A and B form an ideal, regular or quasi-regular solid solution, the entropy of mixing plays a dominant role so that the Gibbs energy reaches the minimum at an equal composition of A and B. The high entropy composition is therefore the optimum composition to suppress the formation of line compounds. (2) If A and B form a sub-regular solution, the Gibbs energy does not reach its minimum at the composition of equal amounts of A and B, even though this composition still offers the highest entropy of mixing. (3) Even in the case that A and B do form an ideal solution, the so-called HEA may still not form due to the existence of other more stable phases. For example, if the Gibbs energy of a line compound sits below the  $a_1b_1$  line in Fig. 1, it will be more stable than the solid solution phase even at the composition with highest

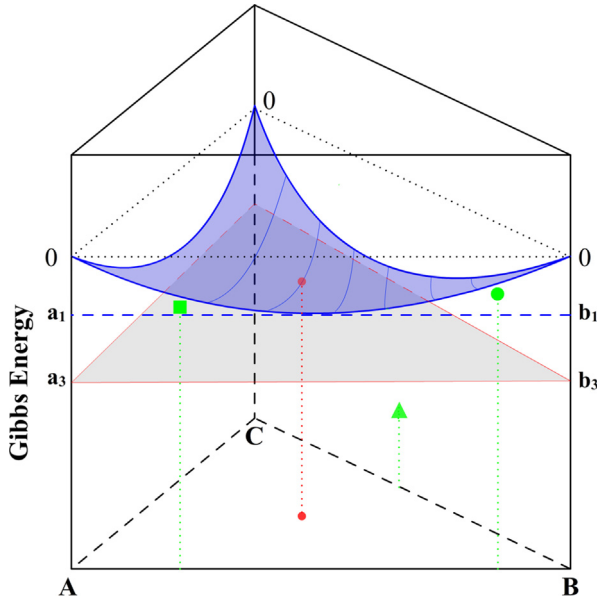


Fig. 2. Gibbs energies of phases in a hypothetical A–B–C system.

entropy of mixing. Although the conclusions above are drawn from a binary system, they are equally applicable to a multi-component system. It should also be pointed out that ideal mixing rarely occurs in a real alloy system.

## 2.2. Ternary A–B–C system

It has been claimed that the high entropy of mixing of disordered phases due to the use of multiple principal components can suppress the intermetallic phases and lead to the formation of simple single-phase microstructure. In this section, we add one more component to the hypothetical A–B binary to form a ternary A–B–C system. We will see what may happen when a new component is introduced to the system and whether it is always beneficial for the development of simple microstructure. Fig. 2 shows the Gibbs energy surface of the disordered *fcc* phase in the ternary A–B–C system. In this case, if the A, B, and C are assumed to form an ideal *fcc* solution phase, the Gibbs energy of this phase can be written as

$$G^{fcc} = x_A G_A^{fcc} + x_B G_B^{fcc} + x_C G_C^{fcc} + RT(x_A \ln x_A + x_B \ln x_B + x_C \ln x_C) \quad (4)$$

Again, if *fcc*-A, *fcc*-B, and *fcc*-C are chosen as the reference states, the Gibbs energy surface is plotted as shown in Fig. 2 which is zero at the three pure components and reaches the minimum in the middle of the Gibbs triangle with equal atomic proportions of the three components. The tangent plane passing the minimum point in the ternary intersects the A–B binary by line  $a_3b_3$ . It is noticed that  $a_3b_3$  sits below  $a_1b_1$ , which means the Gibbs energy of the *fcc* phase is lower due to the addition of a third element. This is easy to understand by comparing Eqs. (2) and (4), in which the position of  $a_1b_1$  is calculated by  $-RT \ln 2$ , while  $a_3b_3$  by  $-RT \ln 3$ . Obviously, *fcc* phase becomes more stable compared to the two binary compounds in the A–B system. However, this does not mean the *fcc* phase becomes more stable in the ternary system. If, for example, there is a very stable compound phase in the B–C binary as shown by the solid triangle in Fig. 2, then adding component C is certainly not favorable for the formation of single-phase *fcc* structure. In case of regular or quasi-regular solutions the shape of the Gibbs energy surface will only be symmetric if the excess Gibbs energies in all three binaries are identical which is practically impossible.

The conclusions obtained with this hypothetical A–B–C ternary, which forms an ideal solution, are: (1) adding one more principal component, C, does increase the entropy of mixing and decrease the Gibbs energy of the disordered solution phase, which is beneficial in suppressing the formation of the binary compounds in the A–B system. (2) If the newly added component leads to the formation of other more stable intermetallic phases in the constituent binaries and stable ternary compounds, the addition of this new element is not beneficial and will lead to the formation of a more complex microstructure.

We intentionally used a very simple hypothetical ternary system in the above discussion for the purpose of illustrating the point that although adding one more key element indeed increases the entropy of mixing of an ideal solution, a single-phase structure is not guaranteed due to the potential formation of other more stable phases. In reality, when a third element is added to a binary system, the following complexities may develop. (1) The disordered phase forms a non-ideal solution. In this case, the minimum of the Gibbs energy surface is not in the middle of the Gibbs triangle, and even though the equal atomic composition still offers the highest entropy of mixing, it is not necessarily the composition that favors the formation of a disordered structure. (2) If there exists a line compound,  $A_{0.75}C_{0.25}$ , in the A–C binary which forms a semi line compound with  $A_{0.75}B_{0.25}$  in the A–B binary, the phase is described as:  $A_{0.75}(B, C)_{0.25}$ , and it may become stable inside the ternary as it also has a contribution from the ideal entropy from mixing B and C atoms. (3) Even though true ternary compound phases are not as common as those in the binary systems, they do exist and play a role in determining the final microstructure. (4) Two or more disordered solid solution phases may form in the same system, which is very common in the real alloy systems. In this case, the entropy of mixing plays the same role in every solid solution phase, and the final microstructure is a result of stability competition among all these phases. Therefore, it is more likely that a mixture of these phases is obtained than a single-phase structure.

In summary, we have illustrated the relative phase stability using a simple hypothetical A–B binary and A–B–C ternary as examples. The real alloy systems can be much more complicated which involve many phases. The microstructure developed in an alloy system depends on many factors, and entropy of mixing is only one of them.

## 3. HEA design aided by phase diagram calculation

A phase diagram is a graphical representation of phase equilibria of a material system in terms of temperature, composition, and pressure (normally fixed at one atmosphere). A phase diagram thus provides an intuitive way of understanding the phase stability, the developed microstructure and the ultimate performance of a material, given alloy composition and temperature. Phase diagrams are therefore widely referred to as road maps for materials design and development.

Traditionally, phase diagrams have been determined purely by experimentation which is costly and time consuming. While the experimental approach is feasible and necessary for the determination of binary and simple ternary phase diagrams, it is less efficient for complicated ternaries, and becomes practically impossible for higher order systems over wide range of composition and temperature. On the other hand, multi-component phase diagrams are needed in the development of commercial alloys since most of them are multi-component in nature. Multi-component phase diagrams are crucial in the development of HEAs since these alloys are based on multiple principal elements with the compositions located in the middle of the multi-dimensional composition

space. Now the question is where to find the multi-component phase diagrams.

Over the past several decades, a phenomenological approach, known as the CALPHAD approach [17–19], has been widely used for the study of phase equilibria of multi-component systems. The essence of this approach is to obtain self-consistent thermodynamic descriptions of the lower order binary and ternary systems, in terms of known thermodynamic data measured experimentally and/or calculated theoretically as well as in terms of the measured phase equilibria. The advantage of this method is that the separately measured phase diagrams and thermodynamic properties can be represented by the same “thermodynamic description” (or called “thermodynamic database”) of a materials system in question. More importantly, on the basis of the known descriptions of the constituent binary and ternary systems, a reliable description of a higher order system can be obtained via an extrapolation method [20]. Model parameters for subsystems higher than ternary are usually not considered in the construction of a multi-component database. This is because interactions between three components are weaker compared to the interactions between two components, and the interactions between even more components are negligibly weak [19,21]. A thermodynamic database developed using this procedure enables us to calculate phase diagrams of the multi-component systems that are experimentally unavailable.

Development of a thermodynamic database for calculating multi-component phase diagrams of HEAs is more challenging than that for traditional alloys. Traditional alloys are mostly based on one key component and the database can be focused at the corner of the key element. The HEAs are based on multiple principal elements; therefore, the database must be valid in the entire composition range. Development of a database containing  $N$  components for the study of HEAs means development of complete thermodynamic descriptions for  $C_N^2$  binary systems and  $C_N^3$  ternary systems. A five-component system consists of 10 binaries and 10 ternaries, a seven-component system consists of 21 binaries and 35 ternaries, and a 10-component system consists of 45 binaries and 120 ternaries. The number of constituent binaries and ternaries is seen to increase rapidly when more than five-component are considered. This makes the development of a complete database for a 10-component system a very ambitious task while the development of a database for a five-component system can be carried out within a reasonable timeframe. This is not only due to the large number of binary and ternary systems that need to be assessed, but also the lack of experimental data that are needed to optimize the model parameters of these systems, especially the ternary systems. It is therefore not very practical to develop a complete thermodynamic database with 10 or more components which can be used to predict the phase equilibria in the middle of composition space. Now the question is: can we still use the CALPHAD approach for the design of alloy with multiple key components?

In this section, we will explore a two-step approach to face this challenge. In the first step, we use binary phase diagrams to identify “matching elements” that are mutually soluble in each other in a certain crystal structure. In the second step, we develop a thermodynamic database for these “matching elements” and use it to identify the composition range where simple single-phase structure may form. This way, we exclude the unfeasible elements first so that development of a complete database for the limited number of “matching elements” is achievable. We will use two alloy systems that were experimentally studied to illustrate the usefulness of this approach.

### 3.1. The Co–Cr–Fe–Mn–Ni system

The CoCrFeMnNi alloy was studied experimentally by Cantor et al. [1] and Otto et al. [16]. Both works observed single-phase *fcc*

structure although an as-cast alloy was studied by Cantor et al. [1] and an annealed microstructure was studied by Otto et al. [16]. The occurrence of a single-phase alloy with equi-atomic composition does not appear likely at first sight in this system since these five components possess four different structures at room temperature. Only Ni is face-centered cubic (*fcc*), Cr and Fe are body-centered cubic (*bcc*), Co is hexagonal close-packed (*hcp*), and Mn

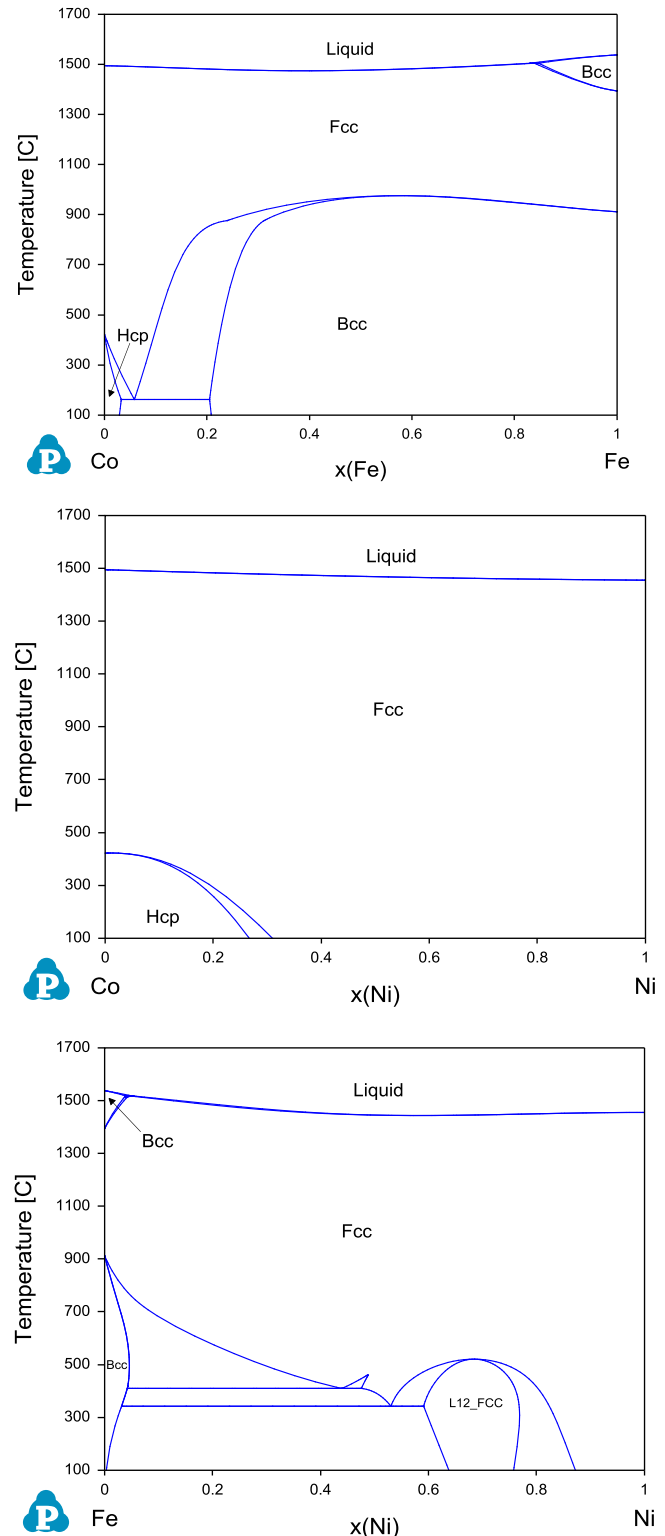


Fig. 3. The three constituent binaries: Co–Fe, Co–Ni, and Fe–Ni in the Co–Fe–Ni ternary system [23].



has an A12 structure. However, after we examine the 10 constituent binary systems of the Co–Cr–Fe–Mn–Ni five-component system, we will find that it is not surprising that single-phase *fcc* microstructure was obtained in their experiments.

The following calculations were carried out by Pandat™ software and its databases [22,23]. Let us start with the Co–Fe–Ni ternary system. Ni possesses an *fcc* structure from room temperature to its melting temperature. Even though Co has *hcp* structure at room temperature, it is *fcc* in the temperature range of 422–1495 °C. Similarly, *fcc* Fe is stable in the temperature range of 911–1394 °C. All the three constituent binaries in this ternary: Co–Fe, Co–Ni, and Fe–Ni, form continuous *fcc* solid solution in a wide temperature range as shown in Fig. 3(a)–(c). These three binary phase diagrams indicate that the single-phase *fcc* structure can be obtained in a wide temperature range when these three elements are mixed together at any ratios, not limited to equal atomic ratio.

When we add Mn into the Co–Fe–Ni system, three more binaries form as shown in Fig. 4(a)–(c). Even though pure *fcc* Mn is stable only in a small temperature range 1087–1138 °C, it forms continuous *fcc* solid solution with Fe and Ni in a wider temperature range. Although Co–Mn does not form continuous *fcc* solid solution, the *fcc* phase is stable in a large temperature range with  $x_{Mn} \leq 0.5$ . Examining the binary phase diagrams of the Co–Fe–Mn–Ni system shown in Figs. 3 and 4, we can conclude that the *fcc* single-phase is stable in a large composition and temperature region in this quaternary system. It is therefore not difficult to obtain a single-phase *fcc* structure when mixing Co, Fe, Mn, and Ni in varying ratios, again not limited to equal atomic ratio.

Now, let us add Cr to this quaternary and form a quinary system. The newly formed constituent binaries are shown in Fig. 5. It is seen that up to a mole fractions of 0.4–0.5 of Cr can be dissolved into *fcc* Co or Ni to form a large stable *fcc* region in the Co–Cr and Cr–Ni binaries, which is not the case for the other two binaries: Cr–Fe and Cr–Mn. In fact, Cr almost has no solubility in *fcc* Mn. It is seen from these four binary phase diagrams that Cr promotes the formation of *bcc* phase, yet there should be a wide temperature and composition region where the *fcc* structure is stable in the Co–Cr–Fe–Mn–Ni quinary system due to the mutual solubility of these elements in the *fcc* phase.

From the 10 binary phase diagrams shown in Figs. 3–5, we reach the conclusion that if development of a simple *fcc* structure is the goal, the Co–Cr–Fe–Mn–Ni quinary is certainly a system with high potential to accomplish the goal. Based on this conclusion, we developed a thermodynamic database for this quinary system to further understand the phase relationship in the middle composition space of this quinary. Fig. 6 shows four isoplethal sections along the Cr–X (X represents Co, Fe, Mn, and Ni) binary, respectively, with the other three elements fixed at a mole fraction of 0.2 each. The purpose is to see how much Cr can be added in the quinary to form the single-phase *fcc* structure. As is seen, the solubility of Cr in the *fcc* phase is quite high at high temperature and decreases with decreasing temperature. For example, if the CoCrFeMnNi (equal atomic proportion of each element) alloy is annealed above 600 °C, a single-phase *fcc* structure will form, while below 600 °C, a mixture of *fcc* and *bcc* phases will form. This is consistent with Otto et al.'s observation [16] who obtained the single-phase *fcc* structure for the alloy annealed at 1000 °C.

Many alloys may show segregation when freezing from the liquid phase. This segregation is the result of slow diffusivities in the solid phase compared to the liquid phase. In this case the composition of the liquid phase no longer corresponds to the equilibrium composition for the given bulk composition and the phase(s) freezing from the liquid also no longer represent equilibrium for the given bulk composition. Only local equilibrium exists at the liquid/solid interface. A simple way to calculate this behavior is the Scheil simulation. For a Scheil simulation, complete

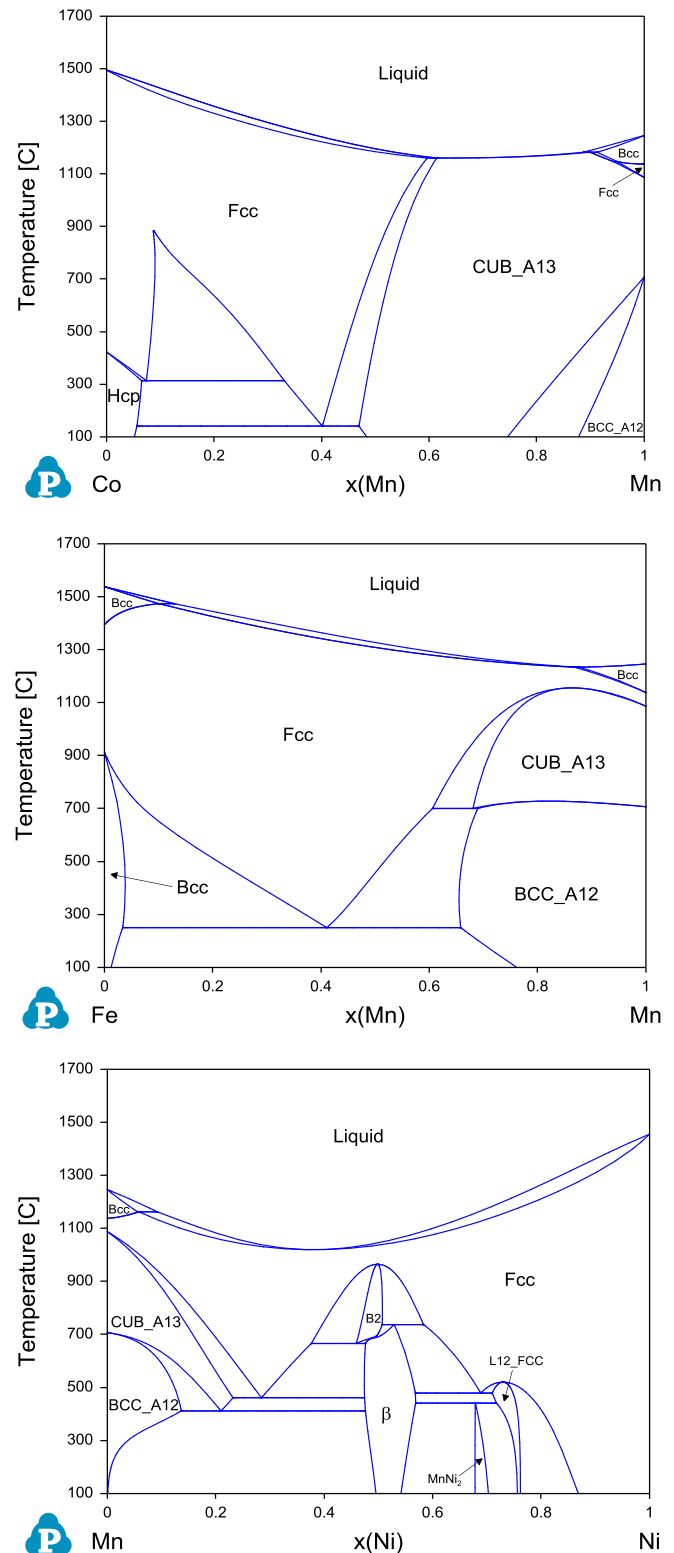


Fig. 4. The three constituent binaries: Co–Mn, Fe–Mn, and Mn–Ni formed by adding Mn into the Co–Fe–Ni ternary to form a quaternary system.

diffusion in the liquid phase, no diffusion in the solid phase(s) and local equilibrium at the liquid/solid interface are assumed to simulate the casting of an alloy. The result of such a Scheil simulation is shown in Fig. 7 for the equi-atomic CoCrFeMnNi alloy. It is seen that the *fcc* phase is the only phase formed during solidification, which is consistent with the experimental observation of Cantor et al. [1].

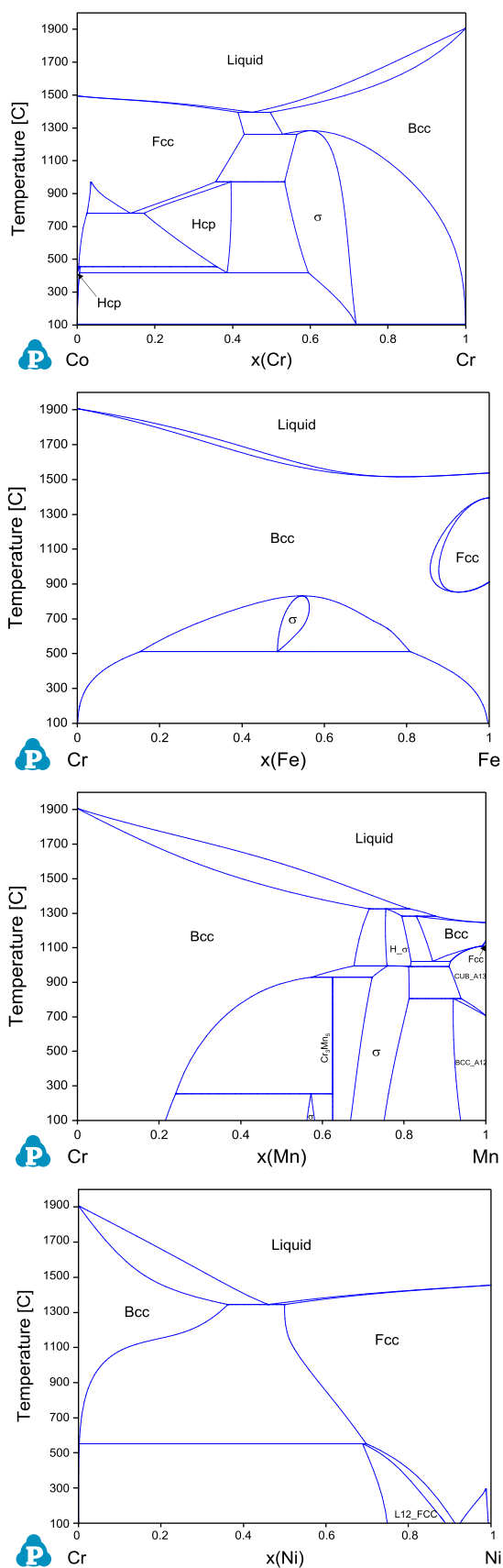


Fig. 5. The four constituent binaries: Co-Cr, Cr-Fe, Cr-Mn, and Cr-Ni formed by adding Cr into the Co-Fe-Mn-Ni quaternary to form a quinary system.

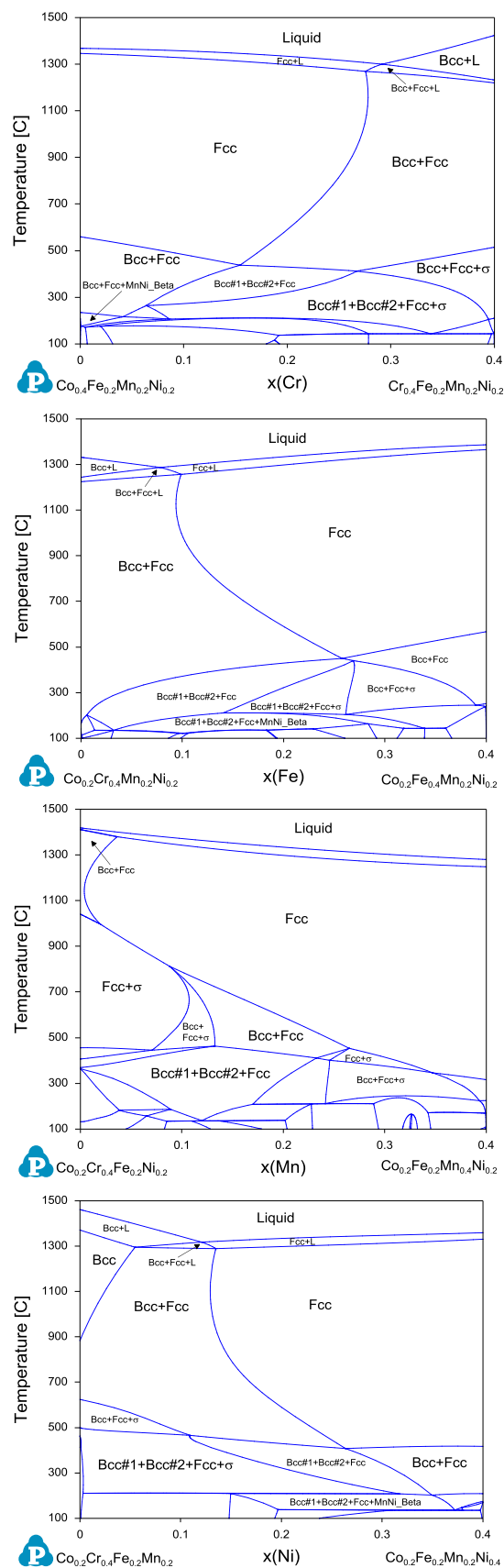


Fig. 6. Isolethal sections parallel to the Cr-X (X represents Co, Fe, Mn, and Ni) binary, respectively, with the other three elements fixed at a mole fraction of 0.2 each.

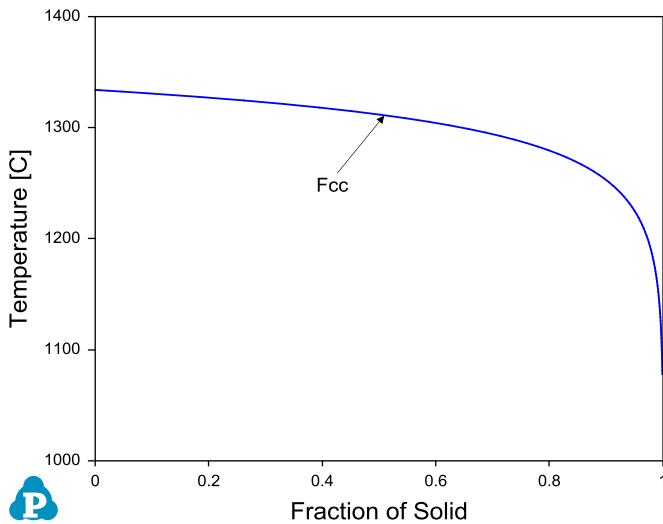


Fig. 7. Scheil simulation of the CoCrFeMnNi alloy with only *fcc* phase solidified.

### 3.2. The Co–Cr–Fe–Mn–Cu system

To prove the point that entropy is not the only factor that determines the phase stability, Otto et al. [16] prepared five other alloys by replacing the Co, Cr, Fe and Ni one at a time using substitution elements with similar properties. They found that none of these five alloys produce single-phase *fcc* structure. One of the alloys is CoCrFeMnCu, i.e., replacing Ni with Cu. Again, let us use phase diagram calculation to see why CoCrFeMnCu is so much different from CoCrFeMnNi. Fig. 8 shows the four binary phase diagrams for the Cu–X (X represents Co, Cr, Fe, and Mn) systems. As is seen these four binaries are quite different from Ni–X (X represents Co, Cr, Fe, and Mn) systems. Each of the four Ni–X binaries has a large field in which the *fcc* phase is stable. On the other hand, Cu tends to form a separate *fcc* phase field, i.e., a miscibility gap occurs when mixing with Cu and Fe. Moreover, Cr almost has no solubility in *fcc* Cu. In these systems the ideal mixing of entropy is not sufficient to compensate for the repulsive interactions between these elements which result in positive excess enthalpies.

Because of the significant differences between the Cu–X and Ni–X binaries, we will expect to get a different result in the middle composition space of the Co–Cr–Fe–Mn–Cu five-component system. Fig. 9 shows two calculated isopleths: one parallel to Cr–Cu, and the other Co–Cr. The other elements are again fixed at a mole fraction of 0.2. As is seen, when CoCrFeMnCu is annealed at 850 °C, a three-phase mixture: *fcc*+*fcc*+*bcc*, will be obtained. A point calculation at this temperature reveals that one of the *fcc* phase enriches Cu ( $x_{Cu}=0.88$ ) and Mn ( $x_{Mn}=0.09$ ), and the other one consists only of a mole fraction of 0.048 of Cu, and mole fractions of 0.2–0.25 of each of the other four elements. This calculated results agree with Otto et al.'s [16] experimental observation fairly well. They found mole fractions of 0.74 of Cu and 0.19 of Mn in the first *fcc*, and a mole fraction of 0.04 of Cu in the second *fcc* for this alloy annealed at 1123 K (850 °C). The difference between the calculation and the Otto et al.'s experiments is that the calculation predicts the formation of *bcc* phase, while Otto et al. believed that the third phase they observed was most likely  $\sigma$  phase.

Note that, the thermodynamic database for the Co–Cr–Cu–Fe–Mn–Ni six-component system was developed at CompuTherm based on the 15 constituent binaries and 20 constituent ternaries. Experimental data for the 15 binary systems are sufficient for the development of thermodynamic descriptions of these binaries, while experimental data for the ternaries are very limited. This database and the calculated phase diagrams (Figs. 6 and 9) need to

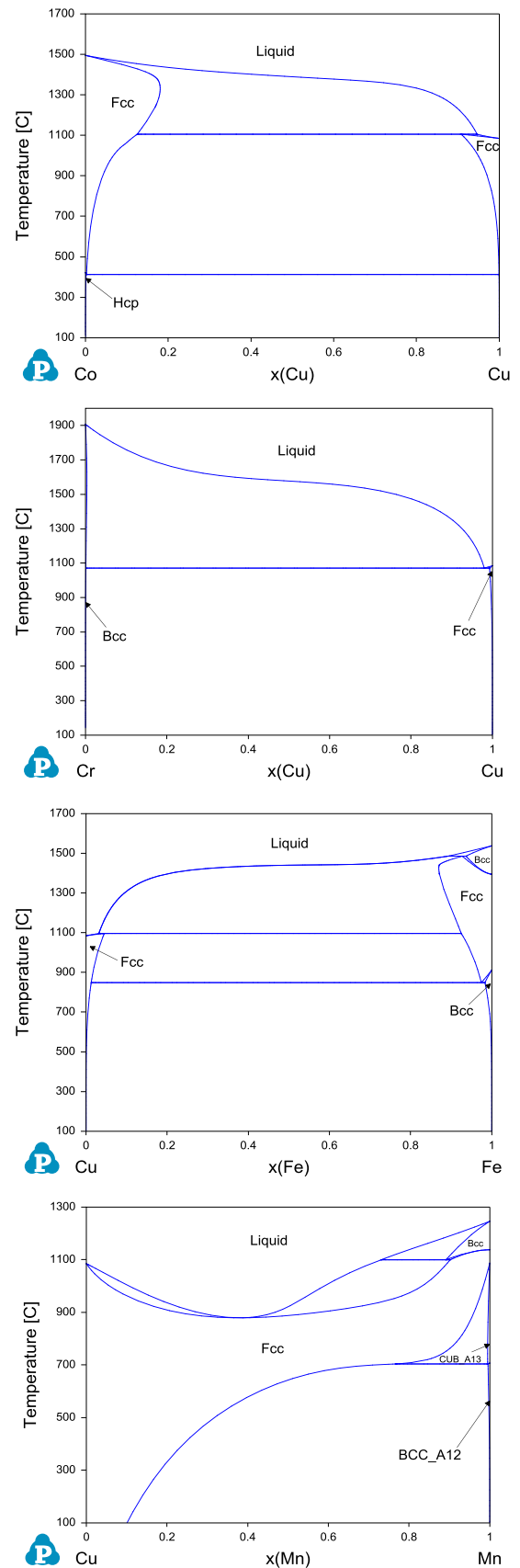


Fig. 8. Cu–X (X represents Co, Cr, Fe, and Mn) binary phase diagrams.

be validated by some key experiments and be further improved. Even though a disordered solution phase in the multi-component system can be well described by the combination of constituent

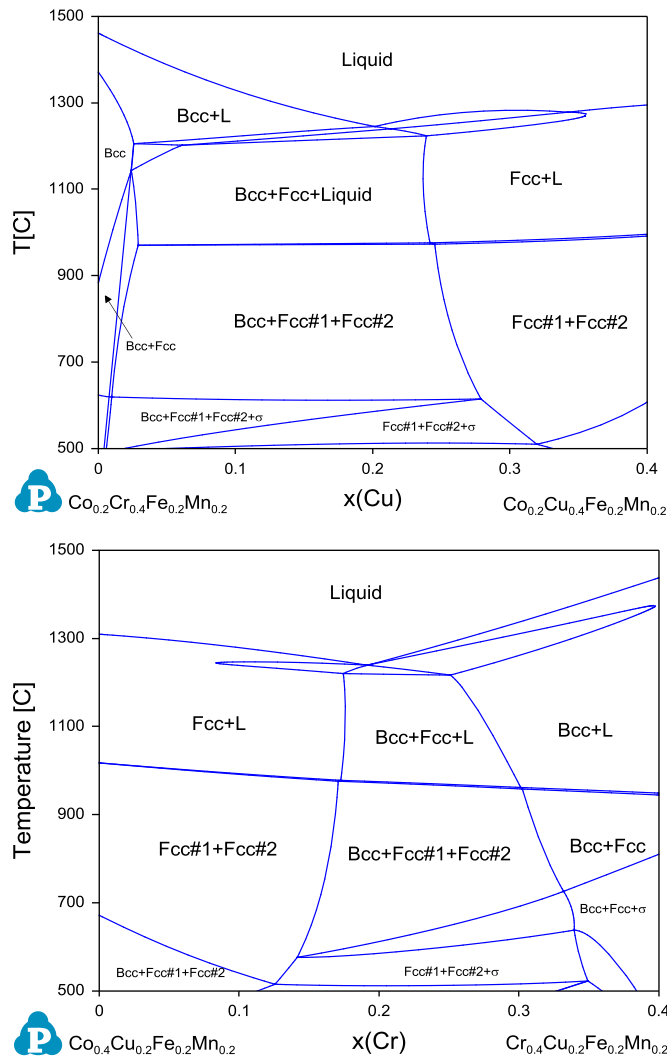


Fig. 9. Isoleths along Cr–Cu and Co–Cr when Ni is replaced by Cu.

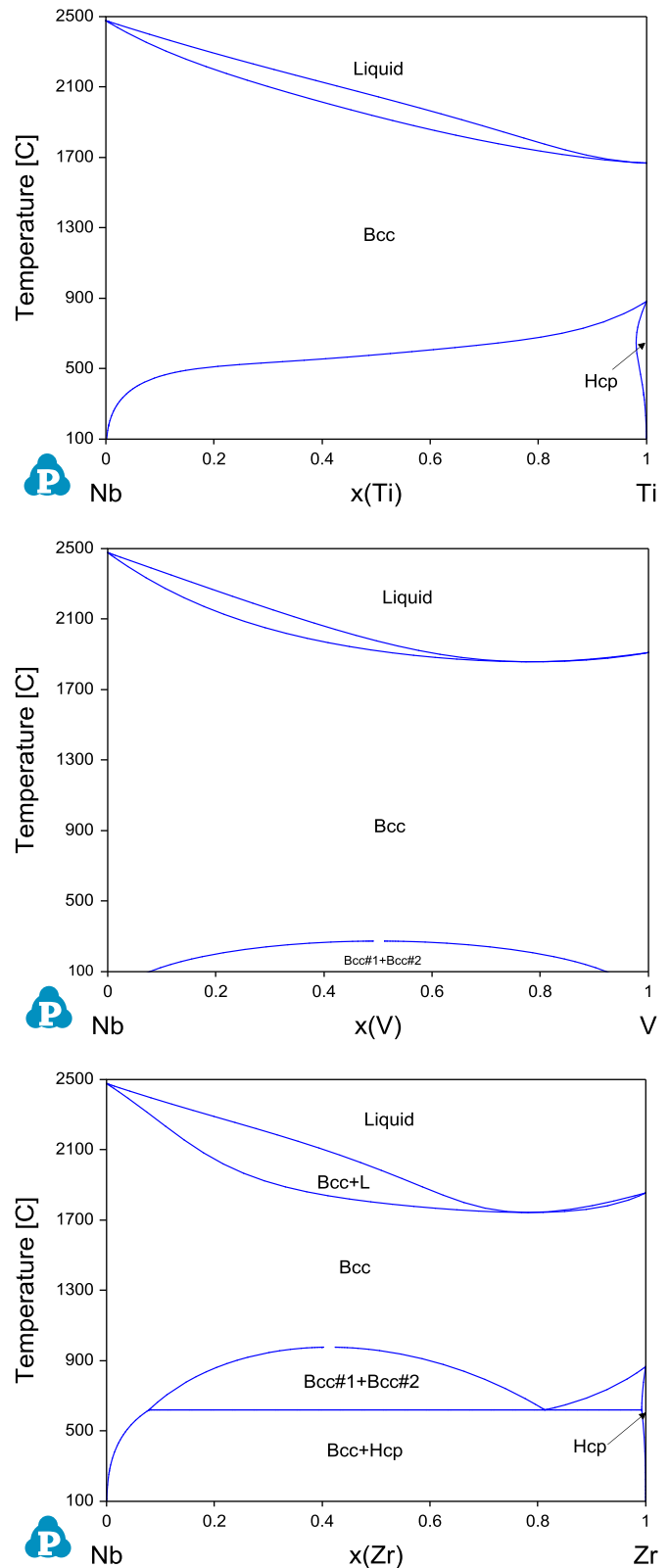


Fig. 10. Phase diagrams of the six binaries in the Nb–Ti–V–Zr quaternary system.

binaries and ternaries via an extrapolation method [20], the composition homogeneity range for the binary or ternary compound phases cannot be well predicted by the extrapolation method. In addition, the CALPHAD approach cannot predict the new phase formed in the higher order systems. With these being said, key experiments should be arranged in the composition ranges where potential HEAs are predicted by the calculations.

### 3.3. The Cr–Nb–Ti–V–Zr system

Recently, Senkov et al. [24] explored the new refractory HEAs based on the Cr–Nb–Ti–V–Zr system and found that NbTiVZr developed a single-phase *bcc* structure and showed good compressive ductility at studied temperatures, while CrNbTiZr and CrNbTiVZr developed a mixture of *bcc*+Laves phases and showed brittle-to-ductile transition between 298 K and 873 K. In this paper, we will demonstrate that this can be understood from phase diagram calculation. The six binary phase diagrams of the Nb–Ti–V–Zr system are shown in Fig. 10. As is seen, the only binary that does not form continuous *bcc* solid solution is the V–Zr system due to the formation of  $V_2Zr$  intermetallic Laves phase which is stable below 1273 °C in this binary. However, there should be a wide temperature and composition range in the Nb–Ti–V–Zr quaternary system where single-phase *bcc* phase is stable. Even though we have not developed a complete thermodynamic

database for this quaternary system, the six constituent binaries have clearly indicated that forming a simple *bcc* structure in this system is not surprising at all.

Now let us add Cr into the Nb–Ti–V–Zr system to see what is going to happen. The four binary phase diagrams formed between Cr and each of the other four elements are shown in Fig. 11. As is



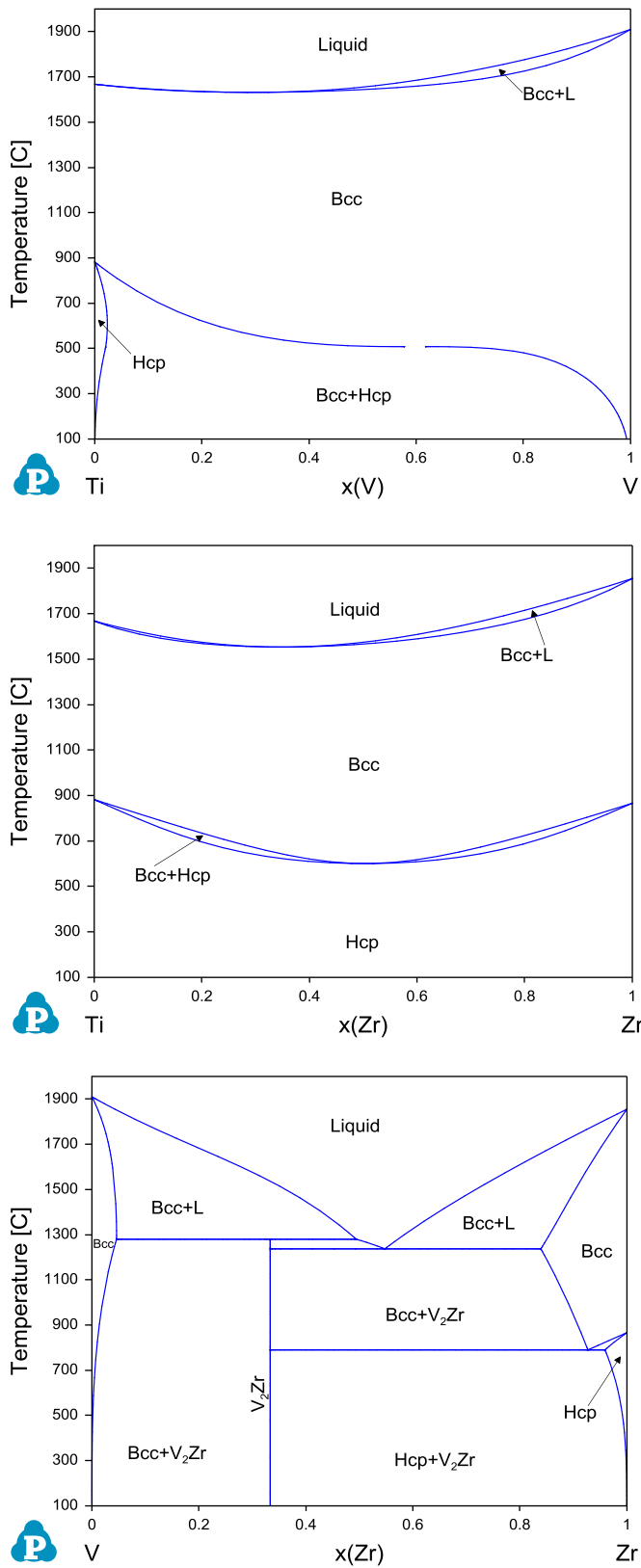


Fig. 10. (continued)

seen, except for the Cr-V binary which forms continuous *bcc* solid solution in the entire composition range, all the other three binaries form Laves phases, including Laves\_C14, Laves\_C15, and Laves\_C36. In the Cr-Nb and Cr-Zr binaries, these Laves phases

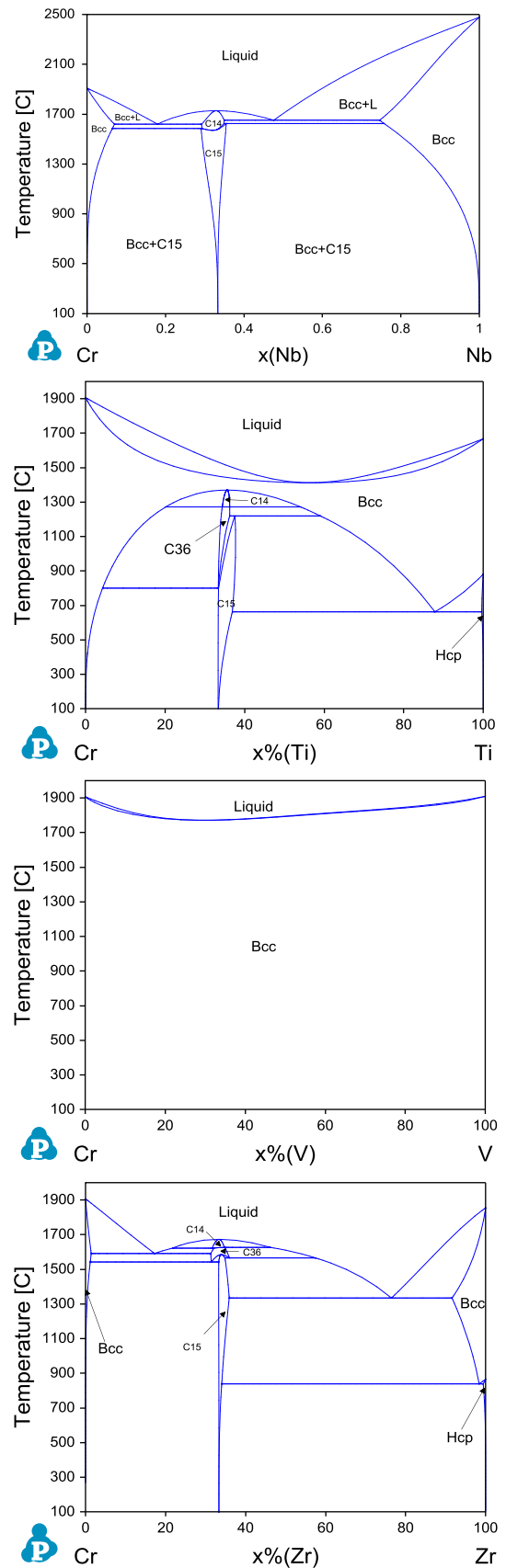


Fig. 11. Phase diagrams of the four binaries of Cr with Nb, Ti, V and Zr.

form at temperatures as high as 1700 °C. This temperature is in the liquid phase field for three of the binaries in the Nb-Ti-V-Zr system, which means these Laves phases are likely to form in the

Cr–Nb–Ti–V–Zr system either from the liquid phase or through a solid phase transformation.

#### 4. Summary and conclusions

The purposes of this paper are twofold: first, to discuss the role of entropy of mixing in the determination of stability of solid solution phases and, second, to discuss the use of the CALPHAD approach in aiding the development of high entropy alloys. The role of entropy of mixing was discussed for both ideal and non-ideal solid solutions using hypothetical systems (binary and ternary). Calculated binary and multi-component phase diagrams are used to understand why HEAs can be developed in some multi-component systems, but not in others. The conclusions we have reached are

- (1) The stability of a phase is determined by its Gibbs energy which includes contributions from both enthalpy and entropy. For a multi-component solid solution phase, the equal-atomic composition represents the state with the highest entropy of mixing but not necessarily the lowest Gibbs energy. The equilibrium state of a system is a result of stability competition among all the phases in the system. Increasing the number of key components does not only increase the entropy of mixing of solid solution phases, but may also lead to the formation of other undesired phases.
- (2) Many so-called high entropy alloys reported in the literature, i. e. a single-phase structure, were obtained by casting. Due to the fast cooling, the major phase observed in the casting microstructure is usually the primary solidified phase, i. e., the matrix phase. If such an alloy is annealed at an elevated temperature or is used in service for a certain length of time, other stable phases may precipitate from the matrix phase.
- (3) The CALPHAD approach, which provides an intuitive way of understanding the phase stability and phase relationship in a multi-component system, has been applied to a broad field of materials design and development. Application of this approach to the design of HEAs is more challenging than that of traditional alloys. This is because traditional alloy design requires a thermodynamic database that covers a limited composition space at the key-element corner, while HEA design requires a database that is valid in the entire composition range. Development of a complete database with 10 or more elements for HEA design is extremely challenging. A two-step approach is proposed in this study to face this challenge. In the first step, binary phase diagrams are calculated to identify “matching elements”, and in the second step,

a thermodynamic database can be developed for the limited number of “matching elements”. This database can then be used to identify the composition range where a simple single-phase structure may form.

- (4) Phase diagrams were calculated for the Co–Cr–Fe–Mn–Ni, Co–Cr–Fe–Mn–Cu, and Cr–Nb–Ti–V–Zr systems using the CALPHAD approach. The calculated binary and multi-component phase diagrams explain the experimentally observed phenomena well.

#### Appendix A. Supplementary material

Supporting data associated with this article can be found in the online version at <http://dx.doi.org/10.1016/j.calphad.2013.10.006>.

#### References

- [1] B. Cantor, I.T.H. Chang, P. Knight, A.J.B. Vincent, *Mater. Sci. Eng. A* 375–377 (2004) 213–218.
- [2] J.W. Yeh, S.K. Chen, S.J. Lin, J.Y. Gan, T.S. Chin, T.T. Shun, *Adv. Eng. Mater.* 6 (5) (2004) 299.
- [3] P.K. Huang, J.W. Yeh, T.T. Shun, S.K. Chen, *Adv. Eng. Mater.* 6 (2004) 74.
- [4] C.J. Tong, Y.L. Chen, S.K. Chen, J.W. Yeh, T.T. Shun, C.H. Tsau, S.J. Lin, S.Y. Chang, *Metall. Mater. Trans. A* 36A (4) (2005) 881.
- [5] U.S. Hsu, U.D. Hung, J.W. Yeh, S.K. Chen, Y.S. Huang, C.C. Yang, *Mater. Sci. Eng. A* 406 (2007) 403.
- [6] G.Y. Ke, S.K. Chen, T. Hsu, et al., *Ann. Chim. Sci. Mater.* 31 (6) (2006) 669.
- [7] P. Lee, Y.Y. Chen, C.Y. Hsu, J.W. Yeh, H.C. Shih, *J. Electrochem. Soc.* 154 (8) (2007) C424.
- [8] Y.J. Zhou, Y. Zhang, Y.L. Wang, G.L. Chen, *Appl. Phys. Lett.* 90 (2007) 181904.
- [9] S. Varalakshmi, M. Kamaraj, B.S. Murty, *J. Alloys Compd.* 460 (2008) 253.
- [10] Y.P. Wang, B.S. Li, M.X. Ren, et al., *Mat. Sci. Eng. A Struct.* 491 (1–2) (2008) 154.
- [11] S.T. Chen, W.Y. Tang, Y.F. Kuo, S.Y. Chen, C.H. Tasu, T.T. Shun, J.W. Yeh, *Mater. Sci. Eng. A* 527 (2010) 5818.
- [12] K.B. Zhang, Z.Y. Fu, *Intermetallics* 22 (2012) 24.
- [13] S. Praveen, B.S. Murty, R.S. Kottada, *Mater. Sci. Eng. A* 534 (2012) 83.
- [14] Y. Zhang, Y.J. Zhou, *Mater. Sci. Forum* 561–565 (2007) 1337.
- [15] S. Guo, C. Ng, J. Lu, C.T. Liu, *J. Appl. Phys.* 109 (2011) 103505.
- [16] F. Otto, Y. Yang, H. Bei, E.P. George, *Acta Mater.* 61 (2013) 2628–2638.
- [17] L. Kaufman, *Computer Calculation of Phase Diagrams*, Academic Press, New York, 1970.
- [18] N., Saunders, A.P. Miodownik, *CALPHAD: A Comprehensive Guide*, in: R.W. Cahn (Ed.), Pergamon Materials Series 1998.
- [19] Y.A. Chang, S.-L. Chen, F. Zhang, X.-Y. Yan, F.-Y. Xie, R. Schmid-Fetzer, W. A. Oates, *Prog. Mater. Sci.* 49 (2004) 313–345.
- [20] K.-C. Chou, Y.A. Chang, *Ber. Bunsenges. Phys. Chem.* 93 (1989) 735.
- [21] U.R. Kattner, *JOM* 49 (12) (1997) 14–19.
- [22] S.L. Chen, W. S. Cao, F. Zhang, Pandat™ software, CompuTherm LLC, Madison WI, USA, (<http://www.compuTherm.com>).
- [23] Certain commercial products are identified in this document. Such identification does not imply recommendation or endorsement by the National Institute of Standards and Technology, nor does it imply that the products identified are necessarily the best available for the purpose.
- [24] O.N. Senkov, S.V. Senkova, C. Woodward, D.B. Miracle, *Acta Mater.* 61 (2013) 1545–1557.